EXPERIMENTAL INVESTIGATION OF THE EFFECTS OF DIFFERENT INSTALLMENT POSITIONS OF AIRFOIL-PROBES ON THE FLOW FIELD OF A COMPRESSOR CASCADE

Ma hongwei / Beihang University

Jin chao / Beihang University

ABSTRACT

Airfoil-probe is a very important measurement technique in the aeroengine compressor experiment. In order to study the impact of different installment positions of the airfoil-probe on the aerodynamic characteristics of the compressor cascade, and reveal the mechanism of the effects of airfoil-probe on the compressor cascade, this paper performed a detail measurement on the downstream flow field of the cascade and the static pressure of the blade surface. The case without the airfoil-probe was referenced as the baseline, and other four cases with the airfoil-probe installed different locations were studied. The results show that the blockage region caused by the airfoil-probe are the main source of the effects of the airfoil-probe. The airfoil-probe reduces the loading of the blade itself and the adjacent blade. The chordwise-installed tube decreases the mass flow of the leakage flow and weakens the intensity of the leakage vortex, but enlarges the influence area. The spanwise tube that is installed at the half chord has the lowest effect on the pressure-side passage, and the nearer the tube is installed to the leading edge, the higher blockage is caused by the tube on the suction-side passage. On conditions that the chordwise-installed tube is installed at the same span, there is an optimum position that can decrease the total pressure loss. The comprehensive influence of the 548 case on the cascade is lowest.

NOMENCLATURE

C	chord length
Cb	blockage coefficient
Cps	static pressure coefficient
Cva	axial velocity coefficient
Cpt	total pressure loss coefficient
Ps	static pressure
$P_{s,in}$	inlet static pressure
P_t	local total pressure
$P_{t,in}$	inlet total pressure
V_a	axial velocity
V_0	inlet velocity
Vorti	axial vortex
V_r	circumferential velocity
V_t	tangential velocity

INTRODUCTION

Airfoil-probe is a very important measurement technique in the aeroengine compressor experiment. Since the 1970s, the airfoil-probe has been applied to aeroengine compressor experiment [1]. As the airfoil-probe installed on the blade surface without the probe support will cause less impact on the flow field. So it is widely used to measure the total pressure and total temperature behind the rotor in the experiments of matching in stages of multistage compressor [2-5]. It is an effective measurement method for matching in stages of multistage compressor. While the airfoil-probe is installed on the blade surface, it necessarily changes the geometry of the blade profile and the flow structure in the vicinity of the blade and downstream. It is significant to decrease the impact of the probe and explore the mechanism of the effect of the probe on the compressor [6-8]. Some studies of the impact of airfoil-probe on the compressor performances have been done.

Xiang, et al. [9] concluded that the error of the performance affected by the airfoil-probe is less than 2% in the axis-compressor engine which has less than 20mm height of the blade through the statistics results. He [10] conducted a flow visualization experiment and 3D numerical simulation on the effects of the airfoil-probes on the aerodynamic performance of an axial compressor, and indicated that the airfoil-probes have a negative influence on the compressor aerodynamic performance at all operating points. And a series of experimental and numerical studies had been conducted on the impact of two different types of airfoil-probes on the compressor performance [11-14].

Stuttgart, Germany
1 - 2 September 2016

The researchers have conducted some studies on the impact of airfoil-probe on the compressor performance as described above, but most of them neglect the influence of the transducer-wire tubes of the airfoil-probe, and rare work has been done on the structure optimization of the transducer-wire tubes of the airfoil-probe. Considering that the local separation characteristics and boundary layer structures must be changed with the different position that the tube is installed, it provides the possibility for the structure optimization of the airfoil. This paper performed a detail measurement on the downstream flow field of the cascade and the static pressure of the blade surface to explore the mechanism of the effects of airfoil-probe on the compressor cascade.

FACILITY AND METHOD

The experimental investigation was carried out in a low-speed cascade wind tunnel in BeiHang University as Fig. 1 shown. The rectangle exit of the outlet tunnel is 400mm× 120mm, and the maximum flow rate is about 1.5 Kg/s. The inlet boundary layers on both the endwalls are less than 3mm. The turbulence intensity at mainstream is 2.6%. The cascade consists of two endwalls and five blades. Those blades are respectively named A, B, C, D, E as shown in Fig. 1. The airfoil-probe is installed on the pressure side of blade C.

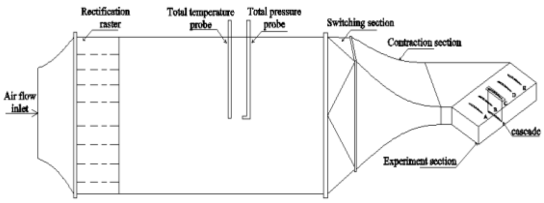

Figure 1 Experimental facility

The specific parameters of the cascade are shown in table 1.The measurement is taken at the Reynolds number of 1.5e5 based on the blade chord and the inlet velocity. The diameter of the tube of the airfoil-probe is 3mm. The installment positions explored include four cases. Fig. 2a shows that the spanwise tube is installed at 50% chord and the chordwise tubes are respectively installed at the 10% span and 50% span, which is named 515 case. Similarity, the case that the spanwise tube is installed at 30% chord and the chordwise tubes are respectively installed at the 45% span and 85% span called 348 (Fig. 2b). Other two cases are 548 (Fig. 2c) and 748 (Fig. 2d). The case without the airfoil-probe is referenced as the baseline.

Table 1 Essential parameters of the cascade

Parameters	value	parameters	value
Number of blade	5	Inlet velocity (m/s)	18.0
Chord length (mm)	126.79	Attack angle (°)	0
Height of cascade (mm)	120	Installment angle (°)	43
Pitch length (mm)	117	Reynolds number	1.5×10^5
Tip clearance (mm)	3.5		

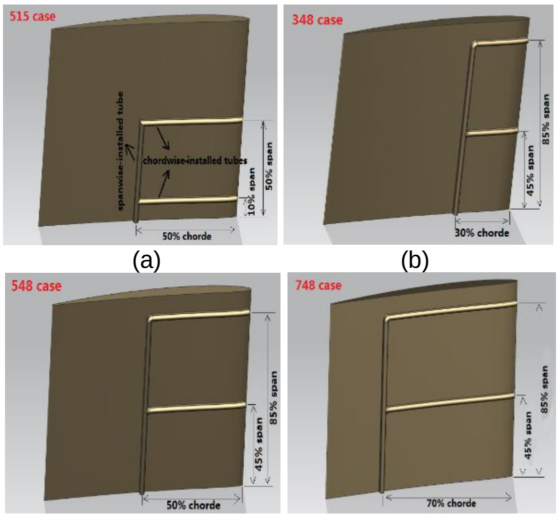

(a) (b)
(c) (d)

Figure 2 Different cases (a) 515 case (b) 348 case (c) 548 case (d) 748 case

The measurement is mainly focus on the downstream flow field and the static pressure on the blade surface. The plane at 25% chord downstream from the trailing edge was measured at 40 spanwise stations and 30 pitchwise stations using a mini five-hole pressure probe. The static pressures of the blade surface are acquired by the static pressure tubes inserted on the blade surface. Those static pressure taps locate at six different spans on the tube: 20% (near blade hub), 50%, 70%, 90%, 95% and 98% (near blade tip) span. There are 15 tubes on the suction surface and 11 tubes on the pressure surface.

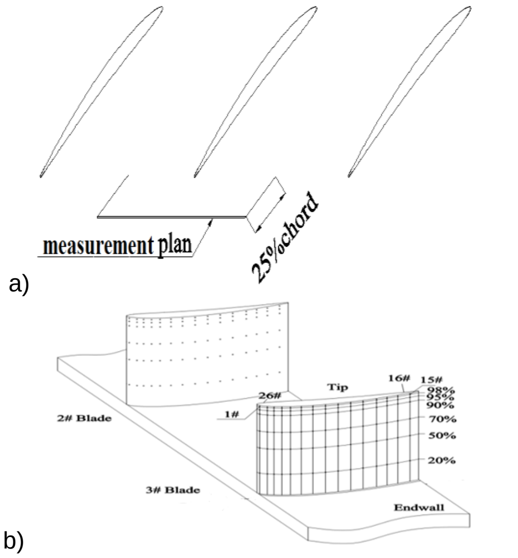

a)
b)

Figure 3 Measurement stations at the outlet and on the blade surface

The mini five-hole probe has a conical head with a diameter of 2 mm is used to measure the downstream flow field of the cascade. All the signals are acquired by the PXIe data acquisition system. And the sampling time is 10s with a sampling frequency of 1 kHz. Before the experiment, the five-hole probe has been calibrated in a calibration tunnel at a range of ±28° yaw angle and ±32° pitch angle, and both at 4° intervals. Through the calibration, the flow angle errors including yaw angle and pitch angle can meet with the experimental requirement within the accuracy of 0.3° by the interpolation on the calibration charts. And the total pressure error is less than 0.5 percent.

RESULTS AND DISCUSSION

As Fig. 4 shows, the high loss regions mainly exist in the wake region, the corner vortex region, the tip leakage flow region and the region that is installed the airfoil-probe. Comparing with the basic case, the losses caused by the tip leakage flow and the corner vortex are higher for all the other cases. Since the blockage of the spanwise-installed tube, there is a low pressure region behind the tube (which can be seen from the distributions of static pressure on the blade surface in Fig.10). Due to this low pressure region, the flow migrates to downward rapidly when it passes by the airfoil-probe. It is the main reason that the position of the high loss region caused by the airfoil-probe is lower than that the tube is installed on the blade.

Because of the migration of the flow described above. In the case of 515, the two high loss regions almost merge into a large one. The interaction of the turbulence induced by the airfoil-probe and the endwall flow causes an evident increase of the total pressure loss at the hub region on the pressure side.

For the cases of 348, 548 and 748, the two high loss regions caused by the chordwise-installed tubes get closer and wider ranging from 348 case to 748 case, which can be explained by that the farther distance that the flow migrated and mixed, the nearer and wider the high loss regions will be.

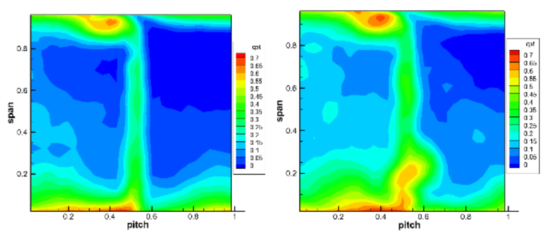

(a) basic case (b) 515 case

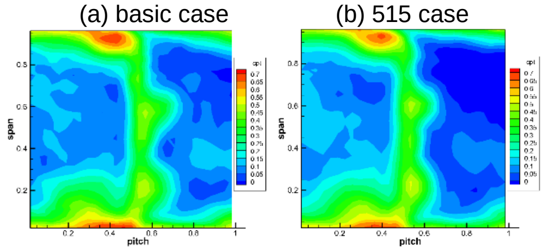

(c) 348 case (d) 548 case

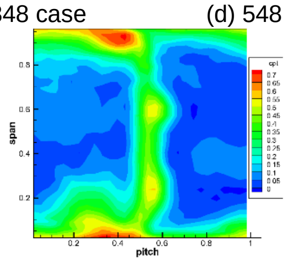

(e) 748 case

Figure 4 Distribution of the total pressure loss coefficien

As Fig. 5 shows, the axial velocity coefficient of the main passage is generally lower than that of the basic case, which indicates that the airfoil-probe decreases the flow capacity of the cascade passage. The distribution of the axial velocity coefficient is similar with that of the total pressure loss coefficient. Low velocity region is in correspondence with the high loss region. Due to the lower installment position of the 515 case, the flow capacity of the corner region on the suction side is worst. For the cases of 348, 548 and 748, the spanwise tube that is installed at the half chord has the lowest effect on the flow capacity of the pressure-side passage, and the nearer the tube is installed to the leading edge, the higher blockage is caused by the tube on the suction-side passage.

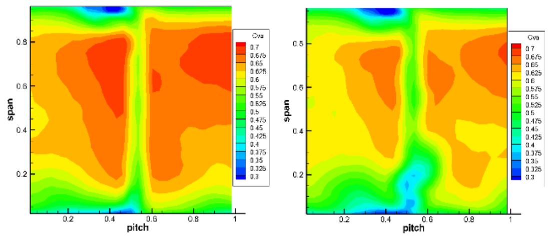

(a) basic case (b) 515 case

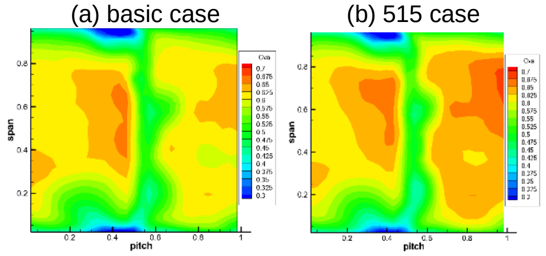

(c) 348 case (d) 548 case

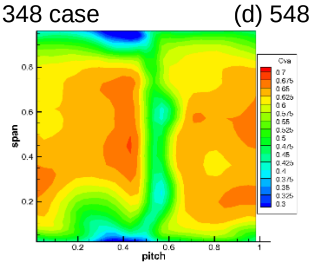

(e) 748 case

Figure 5 Distribution of the axial velocity coefficient

Fig. 6 respectively show the distributions of the pitchwise averaged total pressure coefficient and axil velocity coefficient at different spans. The total pressure loss coefficient increase at less 5% compared with the basic case from 50% span to the 80% span when the airfoil-probes are installed on the blade. In the leakage region, the loss of the 515 case and the 548 case are at the same level and the cases of 348 and 748 are at the higher. The 748 case has the lowest loss level among the cases that installed the airfoil-probe below 50% span, which indicates that the spanwise tube installed close to the trail edge increase the total pressure loss over 60% span, but it benefit to decrease the loss below the 50% span. In other words, there is an appropriate position that the airfoil-probe tube installed on the blade that can make a balance of the loss of the upper span and the lower span to decrease the total pressure loss. The 548 case just meets with this characteristic, and the total pressure loss is indeed lower than other case. The axil velocity coefficient decrease almost 3% compared with the basic case from the 10% span to the 80% span. At the other spans, the differences of the axil velocity coefficient between each cases are not clearly.

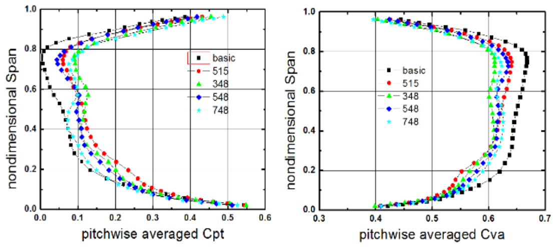

Figure 6 Pitchwise averaged coefficients

As Fig. 7 shows, there are couples of vortex at the measurement plane, which respectively exist at the tip leakage flow region and the region that is installed the airfoil-probes. The low velocity flow induced by the chordwise tube is a streamwise vortex which consists of a pair of contra-rotating vortex. The development of the streamwise vortex has been studied by He Xiang in paper [10]. It also can be seen that the intensity of the leakage vortex of 348, 548, 748 cases are generally lower than that of the basic case, which can be explained by that the tube installed near to the tip region prevents the fluid flowing from the pressure side to the suction side. The low energy fluid near the endwall is rolled into the vortex by the streamwise vortex in the process of flowing downstream. As a result the flow condition is improved at the hub region on the pressure side.

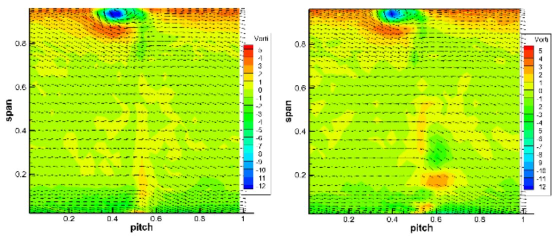
(a) basic case (b) 515 case

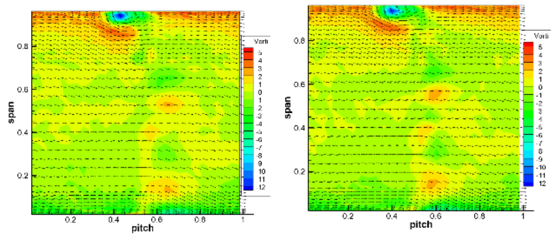
(c) 348 case (d) 548 case

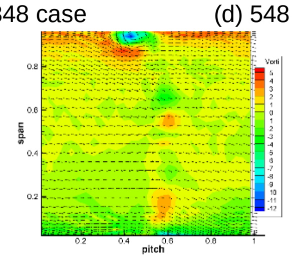
(e) 748 case

Figure 7 Distributions of the axial vortex and the secondary flow vectors

Fig. 8a shows that the high blockage region only exists at the local region that is installed the airfoil-probe. The tip leakage flow and wake almost do not cause any blockage in case of 515. There is also a low negative blockage region at the lower right corner of the plan. This is mainly because that the low energy fluid near the endwall is rolled into the vortex by the streamwise vortex.

For the cases of 348, 548 and 748, the most difference from the 515 case is that the tip leakage flow causes obvious blockage, which indicates that the tube installed near to the tip region decreases the mass flow of the tip leakage flow. The spanwise tube installed at different chord position have a clear effect on the range of high blockage region caused by the chordwise-installed tube.

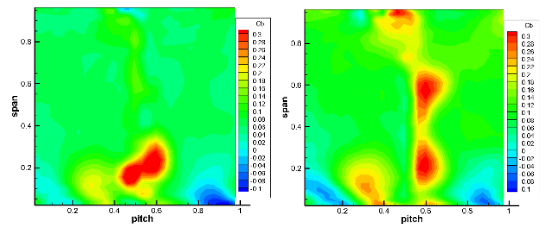
(a) 515 case (b) 348 case

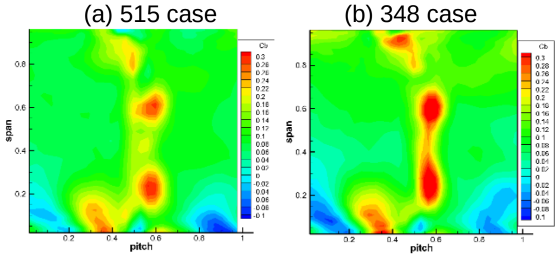
(c) 548 case (d) 748 case

Figure 8 Distribution of the blockage coefficient basing on the basic case

Fig. 9 shows different coefficients of the entire measurement plane. The total pressure loss of the basic case is the lowest and the axial velocity is the highest. For the other cases the high blockage ratio corresponds to the high pressure loss and the low axial velocity. This trend indicates that the blockage region is the main source of the effect of the airfoil-probe on the cascade. The exception is the 515 case shown in Fig. 10d ($\overline{c_{v_a}}$ is ranged as the reverse of c_{v_a}), which causes little blockage but has high total pressure loss level. This is mainly because that the loss caused by the tip leakage flow is high while the tip leakage flow rarely causes any blockage (shown in Fig.9a), which means that the loss caused by the tip leakage flow will stay a high ratio in the mass averaged over the entire measurement plane.

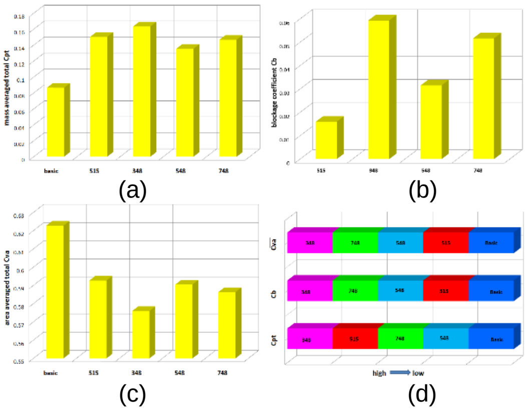

Figure 9 (a) mass averaged total pressure loss (b) blockage coefficient (c) area averaged axial velocity (d) summary table

As the Fig. 10 shows, the airfoil-probe has a clear effect on the static pressure coefficient of the blade itself and the adjacent blade. It reduces the loading of the blade. Due to the blockage of the spanwise-installed tube of the airfoil-probe, there is a high pressure region in front of the tube and a low pressure region behind the tube. The static pressure coefficient increased a lot at the leading edge of the blade on the suction side when the blade installed the airfoil-probes, which indicate that the airfoil induce a blockage in front of the blade on the suction side. The static pressure coefficients on the suction side of the adjacent blade (blade B) shown in Fig.10 (c, e, g, i) are also generally increased compared with the basic case.

For the case of 515, the most difference from the other cases is that the static pressure coefficient of blade C on the pressure side is much higher than other cases at the front edge of the chord over 70% span. It mainly because that the increased blockage in the lower half passage causes an increase in static pressure in the upper. The static pressure on the suction side is also increased comparing with the basic case.

For the cases of 348, 548 and 748, the distributions of the static pressure coefficient on the pressure side follow the trend that it increases first then decreases and then increases. The increase level of the static pressure coefficient corresponds with the position that the spanwise tube installed on the blade. The 348 case has the highest increase level and the 548 case has the lowest. The static pressure on the suction side is also increased comparing with the basic case.

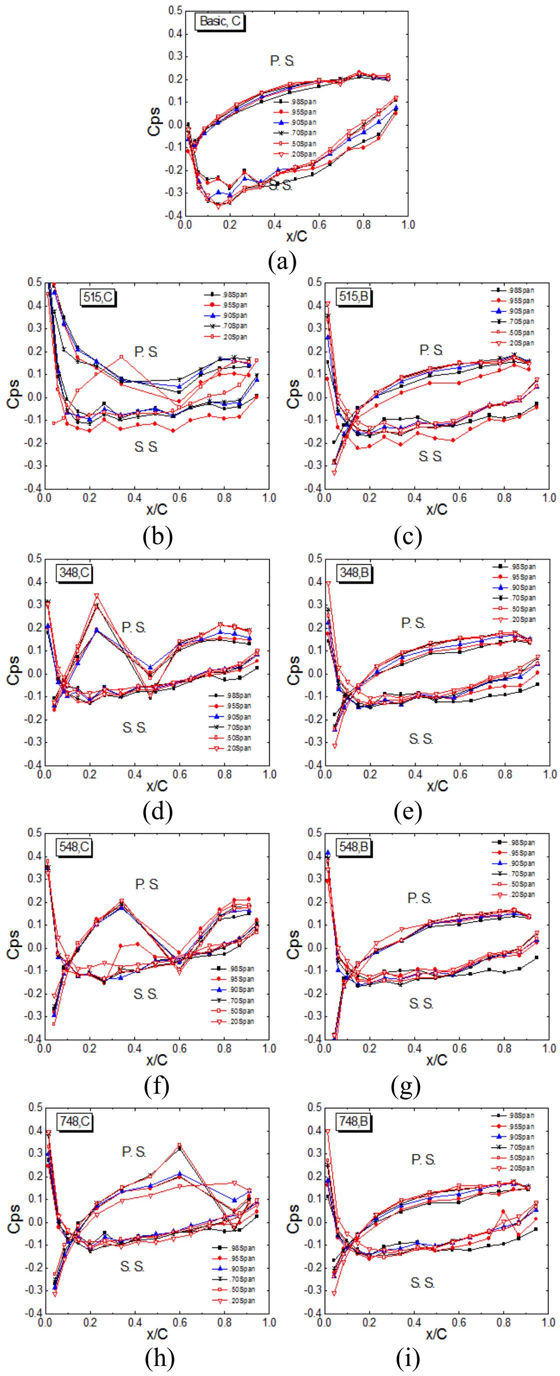

Figure 10 Distributions of the static pressure coefficient

CONCLUSIONS

(1) The blockage region caused by the airfoil-probe are the main source of the effects of the airfoil-probe. The high blockage corresponds to the high pressure loss and the low axial velocity.

(2) The airfoil-probe reduces the loading of the blade itself and the adjacent blade.

(3) The chordwise-installed tube decreases the mass flow of the leakage flow and weakens the intensity of the leakage vortex, but enlarges the influence area.

(4) The spanwise tube that is installed at the half chord has the lowest effect on the pressure-side mass flow capacity, and the nearer the tube is installed to the leading edge, the higher blockage is caused by the tube on the suction-side passage.

(5) On conditions that the chordwise-installed tube is installed at the same span, there is an optimum position that can decrease the total pressure loss. The comprehensive influence of the 548 case on the cascade is lowest.

ACKNOWLEDGMENTS

This investigation was supported by the National Science Foundation of China (Grant No. 51161130525 and No. 51136003), the 111 Project (No. B07009).

REFERENCES

1. Dudzinski T. J. Effect of inlet geometry on flow-angle characteristics of miniature total pressure tubes. NASA-TN-D-6404
2. Biela C., Muller M. W., Schiffer, et al. Unsteady pressure measurement in a single stage axial transonic compressor near the stability limit. *ASME* GT2008-50245
3. Lehmann K. and Happel H. W. Comparison of transonic flow calculations with experimental data. London: *ASME Gas Turbine Conference*, 1982
4. Lecheler S., Schnell R. and Stubert B. Experimental and numerical investigation of the flow in a 5-stage transonic compressor rig. *ASME* 2001-GT-0344
5. Coldrjck S, Lvey P C, Wells R G. The influenc of compressor aerodynamics on pressure probe part1: in rig clibrations. *ASME* 2004-GT-53240,2004
6. Mattevsson H, Langer P, Johansson T, et a1. Design and performance of an efficient high specific power compressor.*ISABE* 2009-1265.2009.
7. Coldrjck S, Lvey P C, Wells R G. The influenc of compressor aerodynamics on pressure probe part2: numerical models. *ASME* 2004-GT-53241,2004
8. Lepicovsky J. Effects of a roting aerodynamic probe on the flow field of a compressor rotor. NASA/CR-2008-215215,2008
9. Xiang H H, Ren M L, Ma H W, et al. Effect of airfoil probes on the experimental results of axial flow compressor performance. *Gas Turbine Experiment and Research*, 2008, 21(3):28-33.[Chinese].
10. HE Xiang, MA Hongwei, REN Minglin, et al. Investigation of the effects of airfoil-probes on the aerodynamic performance of an axial ocmpressor. Chinese Journal of Aeronautics, 2012,25(4):517-523.[Chinese].
11. HE Xiang, MA Hongwei, REN Minglin, et al. Numerical investigation of the effects of an airfoil-probe on flow field in an axial-compressor stator cascade. 20th ISABE conference, 2011, ISABE-2011-1205
12. Xiang H H, Ge N, Ren M L, et al. Comparative investigation of the influence characteristics between two types of airfoil probe in a plane cascade. Gas Turbine Technology 2011; 24(3): 44-49. [Chinese].
13. Xiang H H, Ren M L, Ma H W, et al. Experimental and numerical investigation of airfoil probe influences on the performance of compressor cascade. Gas Turbine Experiment and Research 2010; 23(4): 10-16. [Chinese].
14. Xiang H H, Ren M L, Ma H W, et al. Comparative investigation of two types of airfoil probe effects on flow field in compressor cascade. Gas Turbine Experiment and Research, 2011, 24(3):26-30. [Chinese].
15. Govarhan M, Venkatrayulu N, Vishnubhotla VS. Influence of Tip Clearance on the Inter Blade and Exit Flow Filed of a Turbine Rotor Cascade. ASME Paper 94-GT-359